Spectral and power properties of inline long Josephson junctions

Leonid S. Revin[1,2] and Andrey L. Pankratov[1,2,*]

[1]*Institute for Physics of Microstructures of RAS, GSP-105, Nizhny Novgorod 603950, Russia*

[2]*Laboratory of Cryogenic Nanoelectronics, Nizhny Novgorod State Technical University, Nizhny Novgorod, Russia*

(Received 12 September 2011; revised manuscript received 15 February 2012; published 1 August 2012)

Spectral and power properties of inline long Josephson junctions operating in a flux flow regime are investigated using direct computer simulation of the sine-Gordon equation with a noise source. Good agreement of simulation results with the formula for the linewidth [Pankratov, Phys. Rev. B **65**, 054504 (2002)] is achieved. The comparison with long Josephson junction of overlap geometry is performed. It is demonstrated that the inline junction has the linewidth which is by a factor of 2 larger than the overlap junction, while the maximal oscillation power is roughly the same in spite of the fact that the velocity-matching step height of the inline junction is much smaller than that of the overlap one.

DOI: 10.1103/PhysRevB.86.054501 PACS number(s): 85.25.−j, 05.40.−a

The long Josephson tunnel junction (JTJ) operating in a flux-flow regime is presently considered as the most promising local oscillator (flux-flow oscillator, FFO) for superconducting spectrometers.[1,2] The dynamical properties of the FFO were investigated both experimentally[1–8] and theoretically.[4,9–13] However, the investigation of fluctuational properties of this spatially extended object is restricted by its complexity. For example, there have been discussions about the kink nucleation rate in annular JTJ,[14] which has been resolved only recently by computer simulations.[15] It has been a puzzling problem for more than a decade to find a formula for the spectral linewidth of FFO since it has been known that it is rather large and by roughly one order of magnitude exceeds the linewidth of a short JTJ.[16] This problem has been studied using various theoretical approaches,[17–19] and the formula for the linewidth,[20] taking into account the differential resistance as a function of both bias current and magnetic field, has proven to adequately describe both experimental[5,6] and simulation results.[21,22] Nevertheless, the conversion of bias current fluctuations to magnetic field fluctuations (leading to the linewidth increase) is not yet completely understood.[22,23]

All the above mentioned is related to overlap JTJ, where the bias current flows perpendicular to the long direction of the junction. To our knowledge, the oscillation spectra and the linewidth of long inline JTJ (where the bias current is oriented along the junction) has not been studied either experimentally or theoretically. The only analysis of inline character and comparison for different geometries were devoted to the studies of a single fluxon motion,[24–26] escape from the zero-voltage state,[27] Fiske modes,[4] and the current-voltage (IV) curves.[28,29] However, the study of fluctuational properties of inline JTJ is important not only from a fundamental point of view, but also due to possible applications as a local oscillator, noisy nonstationary spectrometer[30] and magnetic flux sensor.[31] The goal of the present paper is to study the spectral and power properties of inline JTJ versus bias current and noise intensity, and to compare the results with the long overlap JTJ.

It is known that basic properties of the FFO can be described in the frame of the sine-Gordon equation:

$$\phi_{tt} + \alpha\phi_t - \phi_{xx} = \beta\phi_{xxt} + \eta(x) - \sin(\phi) + \eta_f(x,t), \quad (1)$$

where indices t and x denote temporal and spatial derivatives and ϕ is the phase order parameter. Space and time are normalized to the Josephson penetration length λ_J and to the inverse plasma frequency ω_p^{-1}, respectively, $\alpha = \omega_p/\omega_c$ is the damping parameter, $\omega_p = \sqrt{2eI_c/\hbar C}$, $\omega_c = 2eI_cR_N/\hbar$, I_c is the critical current, C is the junction capacitance, R_N is the normal state resistance, β is the surface loss parameter, $\eta(x)$ is the injected current density, normalized to the critical current density J_c, and $\eta_f(x,t)$ is the fluctuational current density. If the critical current density is fixed and the fluctuations are treated as white Gaussian noise with zero mean, its correlation function is $\langle\eta_f(x,t)\eta_f(x',t')\rangle = 2\alpha\gamma\delta(x-x')\delta(t-t')$, where $\gamma = I_T/(J_c\lambda_J)$ is the dimensionless noise intensity, $I_T = 2ekT/\hbar$ is the thermal current, e is the electron charge, $\hbar$ is the Planck constant, k is the Boltzmann constant, and T is the temperature.

It is well known that the mode of the current injection into the Josephson junctions can affect their static and dynamic properties.[16] For the overlap geometry most theoretical models have assumed uniform distribution of the bias current along the junction length. However, in a long narrow JTJ the current distribution is essentially nonuniform, having singularities at the junction edges.[16,32] In the inline case, where the bias current is injected into the junction parallel to its long direction (which in the one-dimensional model leads to injection at the ends of the junction only), the dynamic picture is quite different. Various junction geometries provide the following current distributions $\eta(x)$[32]:

$$\begin{aligned} \eta_{\rm un}(x) &= \eta_0 && \text{(uniform)},\\ \eta_{\rm ov}(x) &= (\eta_0 L/\pi)/\sqrt{x(L-x)} && \text{(mixed)}\\ \eta_{\rm in}(x) &= \eta_0 L[\delta(x)+\delta(x-L)] && \text{(inline)}, \end{aligned} \quad (2)$$

where η_0 is the total current in the film. The boundary conditions simulating RC loads, see Refs. 9, 11, 21, and 22, are

$$\phi_x(0,t) + r_Lc_L\phi_{xt}(0,t) - c_L\phi_{tt}(0,t) + \beta r_Lc_L\phi_{xtt}(0,t) + \beta\phi_{xt}(0,t) = \Gamma, \quad (3)$$

$$\phi_x(L,t) + r_Rc_R\phi_{xt}(L,t) + c_R\phi_{tt}(L,t) + \beta r_Rc_R\phi_{xtt}(L,t) + \beta\phi_{xt}(L,t) = \Gamma, \quad (4)$$

here Γ is the normalized magnetic field, and L is the dimensionless length of the FFO in units of λ_J. The dimensionless capacitances and resistances $c_{L,R}$ and $r_{L,R}$

are the FFO RC load placed at the left and at the right ends, respectively. Note that in the inline case the bias current distribution of Eq. (2) can be accounted for in the boundary conditions instead of the sine-Gordon equation (1), where the term $\eta(x)$ is absent [for brevity here we do not write the surface losses and RC-load system as it is done in Eqs. (3) and (4)]: $\phi_x(0,t) = \Gamma - \eta_0 L/2$, $\phi_x(L,t) = \Gamma + \eta_0 L/2$.

At high magnetic fields a dense chain of vortices under the influence of a bias current is moving unidirectionally through the junction. This fluxon train continuously penetrates from one edge of the junction and radiates at the other. In the overlap JTJ permanent influence of the Lorentz force is maintained through the distributed bias current, while in the inline geometry the fluxons receive an accelerating input due to $\eta_{\rm in}$ near the two junction ends only. Away from the junction edge this inline current influence decreases and for larger damping coefficients this effect is reduced more rapidly. As for a single fluxon motion,[25,32] we can crudely estimate the dependence of the FFO regime established for a different junction parameter using the following terms: In the case $\alpha L \ll 1$ the FFO regime in the inline JTJ is similar to the overlap case. If $\alpha L \geqslant 1$ the current-voltage dependence as well as spectral properties become different for various bias feeds Eq. (2).

The computer simulations are performed at the same parameters as in work[21]: $\alpha = 0.033$, $\beta = 0.035$, $\Gamma = 3.6$, $c_L = c_R = 100$, $r_R = 2$, $r_R = 100$, but for lower noise intensity $\gamma = 0.05$. First let us consider a rather short JTJ with $L = 5$. The IV curves we obtained were similar to the results of Ref. 22. They demonstrate distinct Fiske steps (smoothed at larger lengths due to smaller distance between the steps and effect of load and surface losses[11]) which leads to complex nonmonotonic behavior of the spectral linewidth, see Fig. 1. The power spectral density of FFO is computed as Fourier transform of the correlation function of the second kind $\Phi[\tau] = \frac{1}{T_{\rm av}} \int_0^{T_{\rm av}} \langle v_0(t) v_0(t+\tau) \rangle \, dt$, where $v_0(t) = d\phi(t,0)/dt$ is the voltage at the RC load ($x = 0$) and $T_{\rm av}$ is the averaging time. The spectral linewidth is then defined as full width at

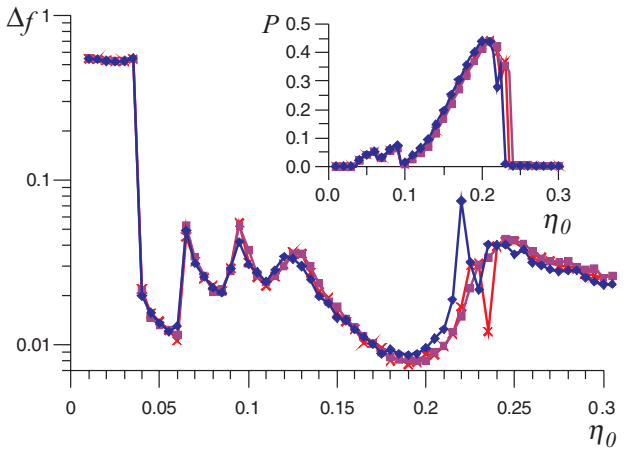

FIG. 1. (Color online) FFO linewidth versus total bias current, computed for $L = 5$ and different $\eta(x)$, see Eq. (2): Curve with rectangles corresponds to uniform distribution of overlap geometry $\eta_{\rm un}$, curve with crosses corresponds to mixed overlap $\eta_{\rm ov}$, and curve with diamonds corresponds to inline $\eta_{\rm in}$. Inset: Radiated power from the end $x = 0$ versus η_0, the notations are the same as for the linewidth.

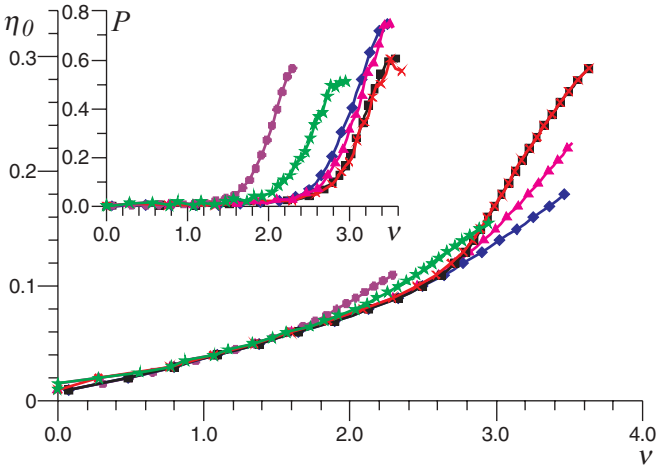

FIG. 2. (Color online) The IV curves of loaded FFO. Uniform overlap (curves coincide): $L = 20$ (curve with crosses) and $L = 40$ (curve with rectangles); mixed overlap: $L = 20$ (curve with triangles) and $L = 40$ (curve with diamonds); and inline: $L = 20$ (curve with stars) and $L = 40$ (curve with circles). Inset: FFO power versus voltage, the notations are the same as for IV curves.

half maximum. The FFO linewidth for different bias current profiles is presented in Fig. 1, while the power at RC load is the inset of Fig. 1. Here the power falls down at bias currents around $\eta_0 \approx 0.23$ due to a jump from the Fiske step to the ohmic line. As discussed above, if $\alpha L < 1$, the FFO regimes are the same for all junctions with similar spectral and power characteristics.

Now let us consider a more interesting case of a long junction $\alpha L > 1$. The IV curves for different junction geometries and $L = 20$, $L = 40$ are presented in Fig. 2. As it has been shown in Ref. 33, for uniform current distribution, that the dependence of the flux-flow step height η_{0h} on the normalized junction length L is nonlinear: For small lengths the step height η_{0h} increases with L and then becomes almost constant. As one can see from Fig. 2, the IV curves for current density $\eta_{\rm un}$ actually coincide. While for mixed overlap and inline cases the step heights for $L = 20$ are larger than for $L = 40$, that is, from certain L values an increase of junction length leads to a decrease of step heights. However, contrary to the step height, the maximal radiation power for the inline JTJ increases with an increase of the length (at least up to $L = 80$), while for overlap junctions it remains the same starting from $L = 20$, see the inset of Fig. 2.

Now let us look at the spectral and power characteristics for junctions with $L = 40$. The largest signal is obtained biasing the junction near the top of the flux-flow branch $\eta_0 = \eta_{0h}$. Although the step height for various junction geometries is different, the maximum radiated power for all three cases is almost the same and corresponds to their own η_{0h}, see the inset of Fig. 3. The linewidths of the FFOs at the largest signal are $\Delta f_{\rm un} = 0.0179$, $\Delta f_{\rm ov} = 0.0133$, $\Delta f_{\rm in} = 0.0247$, while the minimal attainable linewidths are $\Delta f_{\rm un} = 0.0094$, $\Delta f_{\rm ov} = 0.0133$, $\Delta f_{\rm in} = 0.0243$. So, for the inline JTJ the linewidth is 2–2.5 times larger than for the overlap uniform and mixed current distributions. Therefore, the inline junctions seem to be more suitable as a source

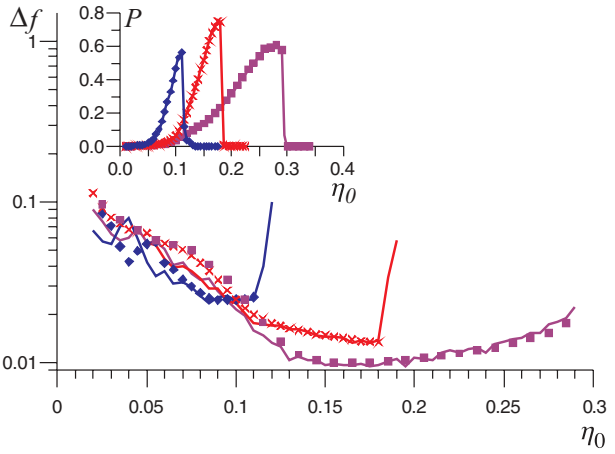

FIG. 3. (Color online) The FFO linewidth for $L = 40$ and different junction geometries: Uniform overlap [violet curve and rectangles, simulations and theory (5)], mixed overlap [red curve and crosses, simulations and theory (5)], and inline [blue curve and diamonds, simulations and theory (5)]. The inset: The radiated power (simulations) for the same geometries.

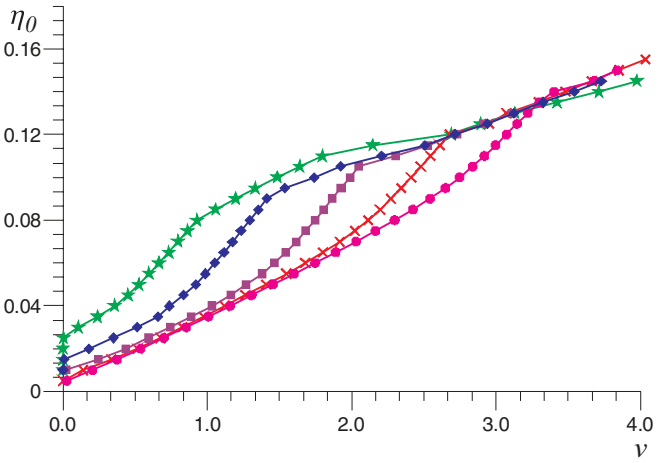

FIG. 4. (Color online) The IV curve of loaded FFO, inline geometry $L = 40$. Curve with stars $\Gamma = 1.5$, curve with diamonds $\Gamma = 2.2$, curve with rectangles $\Gamma = 3.2$, curve with crosses $\Gamma = 4.2$, and curve with circles $\Gamma = 5.2$.

for noisy nonstationary spectrometers.[30] Since an autonomous FFO has a perfectly Lorentzian spectral line[5,22] (arising due to the diffusion of phase of the emitted signal), it provides an opportunity to apply the FFO for development of Fourier spectroscopy in microwave and THz ranges[30]: The phase-diffusion field at short times acts like a coherent one, inducing macroscopic polarization in quantum systems. Thus, one can combine advantages of pulsed and coherent sources, that is, the Lorentzian line shape of molecule emitted signals and broadband measurements in one shot without a complicated phase lock loop system required for coherent sources.

The formula for the FFO linewidth of Ref. 20, which in addition to conventional differential resistance over bias current $r_d = dv/d\eta_0$ takes into account the differential resistance over magnetic field $r_d^{CL} = Ldv/d\Gamma$,

$$\Delta f_{\mathrm{FFO}} = 2\alpha\gamma\left(r_d + \sigma r_d^{CL}\right)^2/L, \tag{5}$$

demonstrates good agreement with the experiment,[5,6] and with simulation results for overlap junctions.[21,22] In Fig. 3 the results of computer simulations of the linewidth for different bias feeds are compared with the theory (5) with the only fitting parameter σ, fixed for each curve [violet curve and rectangles, simulations and theory (5) with $\sigma = 0.205$ for uniform overlap bias; red curve and crosses, simulations and theory (5) with $\sigma = 0.1$ for mixed overlap bias; and blue curve and diamonds, simulations and theory (5) with $\sigma = 0.4$ for inline bias]. One can see that theory (5) agrees well with the simulation results for all three cases. Certain disagreement in the area of small and large η_0 occurs due to the impossibility to correctly calculate r_d^{CL} away from the flux flow step, where the IV curves for different values of Γ actually coincide. The fitted values of σ allow estimation of r_d and σr_d^{CL} contributions $m = \sigma r_d^{CL}/r_d$ for different designs: $m_{\mathrm{un}} \approx 1.3$ for uniform distribution, $m_{\mathrm{ov}} \approx 0.18$ for mixed case, but for the inline case $m_{\mathrm{in}} \approx 0.4$ increases again. So, the mixed case demonstrates minimal contribution of magnetic field fluctuations, which (in spite of twice larger r_d) results in the minimal linewidth at the largest emitted power, see Fig. 3.

It is well known[1–3,11] that in the overlap JTJ reducing of the magnetic field ($\Gamma \leqslant 2.5$) leads to transformation of the flux-flow regime into Fiske steps, complicating continuous frequency tuning. In Fig. 4 the IV curves for inline junction $L = 40$ are presented versus the external magnetic field Γ. The FFO regime is stored in the broad range $\Gamma \geqslant 1.5$ (the Fiske steps are almost invisible even in the limit of vanishing noise intensity, allowing continuous frequency tuning) and the minimal linewidth for each Γ in the working areas is roughly the same, see Fig. 5. The maximum radiated power slightly varies versus Γ and the largest signal corresponds to $\Gamma \approx 3.2$.

The influence of noise on the FFO spectral properties is estimated by plotting the minimal attainable linewidth and the maximal power for different current distributions, see Fig. 6. It is seen that the noise in inline JTJ leads to larger

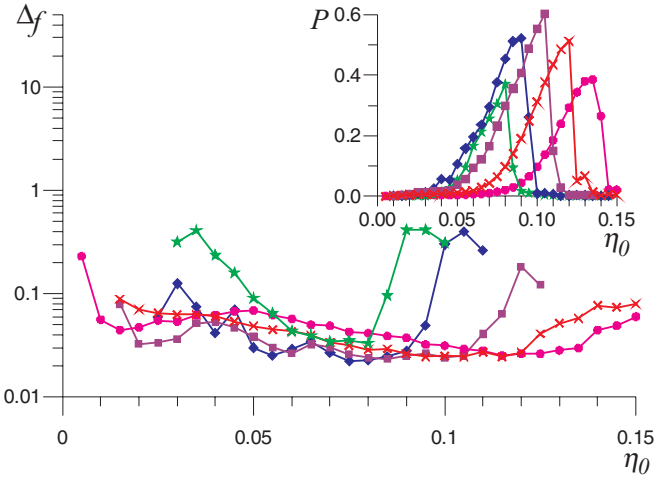

FIG. 5. (Color online) Linewidth and radiated power (the inset) of the inline FFO, $L = 40$. Curve with stars $\Gamma = 1.5$, curve with diamonds $\Gamma = 2.2$, curve with rectangles $\Gamma = 3.2$, curve with crosses $\Gamma = 4.2$, and curve with circles $\Gamma = 5.2$.

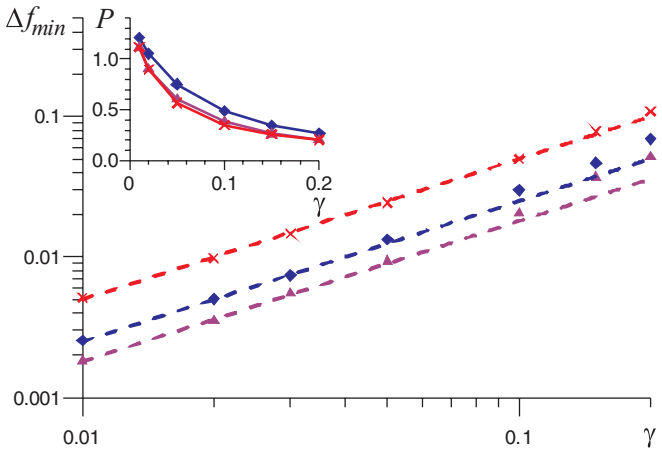

FIG. 6. (Color online) Minimal attainable linewidth and maximal radiated power (the inset) for $L = 40$, $\Gamma = 3.6$, and different junction geometries: Uniform overlap (curve with triangles), mixed overlap (curve with diamonds), and inline (curve with crosses). Dashed lines are linear fit to computed data.

linewidth in comparison with overlap junctions. For uniform and mixed overlap cases the slopes of $\Delta f_{\min}(\gamma)$ are 0.18γ and 0.25γ, respectively, while for inline junction it corresponds to 0.5γ dependence. The deviation from linear dependence of the linewidth starts from $\gamma \geqslant 0.1$. Behavior of the radiated power is strictly nonlinear: For all geometries it sharply decreases by a factor of 3 for $\gamma = 0.1$ compared with $\gamma = 0.01$.

In conclusion, the spectral and power properties of a long inline Josephson tunnel junction have been studied by numerical solution of the one-dimensional sine-Gordon equation with noise source, taking into account surface losses and RC load. The distinct behavior of inline and overlap junctions with changing the external magnetic field and noise intensity is shown. Good agreement of simulation results with the formula for the linewidth (5) is achieved. It is demonstrated that the inline junction has the linewidth which is by a factor of 2 larger than the overlap junction, while the maximal oscillation power is roughly the same in spite of the fact that the height of the velocity-matching step of the inline junction is much smaller than that of the overlap one.

The work was supported by RFBR Project No. 09-02-00491, Human Capital Foundation, Dynasty Foundation and by the Act 220 of Russian Government (project 25).

*alp@ipm.sci-nnov.ru

[1] T. Nagatsuma, K. Enpuku, F. Irie, and K. Yoshida, J. Appl. Phys. **54**, 3302 (1983); **56**, 3284 (1984); **58**, 441 (1985); **63**, 1130 (1988).
[2] V. P. Koshelets and S. V. Shitov, Supercond. Sci. Technol. **13**, R53 (2000).
[3] V. P. Koshelets, S. V. Shitov, A. V. Shchukin, L. V. Filippenko, J. Mygind, and A. V. Ustinov, Phys. Rev. B **56**, 5572 (1997).
[4] M. Cirillo, N. Grønbech-Jensen, M. R. Samuelsen, M. Salerno, G. V. Rinati, Phys. Rev. B **58**, 12377 (1998).
[5] V. P. Koshelets, P. N. Dmitriev, A. B. Ermakov, A. S. Sobolev, A. M. Baryshev, P. R. Wesselius, and J. Mygind, Supercond. Sci. Technol. **14**, 1040 (2001).
[6] V. P. Koshelets, P. N. Dmitriev, A. S. Sobolev, A. L. Pankratov, V. V. Khodos, V. L. Vaks, A. M. Baryshev, P. R. Wesselius, and J. Mygind, Physica C **372**, 316 (2002); **376**, 316 (2002).
[7] V. P. Koshelets, S. V. Shitov, L. V. Filippenko, P. N. Dmitriev, A. B. Ermakov, A. S. Sobolev, M. Yu. Torgashin, A. L. Pankratov, V. V. Kurin, P. Yagoubov, and R. Hoogeveen, Supercond. Sci. Technol. **17**, S127 (2004).
[8] V. P. Koshelets, P. N. Dmitriev, A. B. Ermakov, A. S. Sobolev, M. Yu. Torgashin, V. V. Kurin, A. L. Pankratov, and J. Mygind, IEEE Trans. Appl. Supercond. **15**, 964 (2005).
[9] C. Soriano, G. Costabile, and R. D. Parmentier, Supercond. Sci. Technol. **9**, 578 (1996).
[10] M. Jaworski, Phys. Rev. B **60**, 7484 (1999).
[11] A. L. Pankratov, A. S. Sobolev, V. P. Koshelets, and J. Mygind, Phys. Rev. B **75**, 184516 (2007).
[12] M. Jaworski, Supercond. Sci. Technol. **21**, 065016 (2008).
[13] M. Jaworski, Phys. Rev. B **81**, 224517 (2010).
[14] P. Hanggi, F. Marchesoni, and P. Sodano, Phys. Rev. Lett. **60**, 2563 (1988); M. Buttiker and T. Christen, *ibid.* **75**, 1895 (1995); P. Hanggi and F. Marchesoni, *ibid.* **77**, 787 (1996); M. Buttiker and T. Christen, *ibid.* **77**, 788 (1996).
[15] K. G. Fedorov and A. L. Pankratov, Phys. Rev. Lett. **103**, 260601 (2009).
[16] K. K. Likharev, *Dynamics of Josephson Junctions and Circuits* (Gordon and Breach, New York, 1986); A. Barone and G. Paterno, *Physics and Applications of the Josepson Effect* (Wiley, New York, 1982).
[17] A. A. Golubov, B. A. Malomed, and A. V. Ustinov, Phys. Rev. B **54**, 3047 (1996).
[18] A. P. Betenev and V. V. Kurin, Phys. Rev. B **56**, 7855 (1997).
[19] M. Salerno, M. R. Samuelsen, and A. V. Yulin, Phys. Rev. Lett. **86**, 5397 (2001).
[20] A. L. Pankratov, Phys. Rev. B **65**, 054504 (2002).
[21] A. L. Pankratov, Appl. Phys. Lett. **92**, 082504 (2008).
[22] A. L. Pankratov, Phys. Rev. B **78**, 024515 (2008).
[23] J. Mygind, V. P. Koshelets, M. Samuelsen, and A. S. Sobolev, IEEE Trans. Appl. Supercond. **15**, 968 (2005).
[24] O. A. Levring, N. F. Pedersen, and M. R. Samuelsen, Appl. Phys. Lett. **40**, 846 (1982).
[25] O. A. Levring, N. F. Pedersen, and M. R. Samuelsen, J. Appl. Phys. **54**, 987 (1982).
[26] N. F. Pedersen and A. Davidson, Phys. Rev. B **41**, 178 (1990).
[27] M. G. Castellano, G. Torrioli, C. Cosmelli, A. Costantini, F. Chiarello, P. Carelli, G. Rotoli, M. Cirillo, and R. L. Kautz, Phys. Rev. B **54**, 15417 (1996).
[28] P. Cikmacs, M. Cirillo, V. Merlo, and R. Russo, IEEE Trans. Appl. Supercond. **11**, 99 (2001).
[29] K. Yoshida, T. Nagatsuma, K. Sueoka, K. Enpuku, and F. Irie, IEEE Trans. Magn. **21**, 899 (1985).
[30] E. A. Sobakinskaya, A. L. Pankratov, and V. L. Vaks, Phys. Lett. A **376**, 265 (2012).
[31] R. Monaco, J. Mygind, and V. P. Koshelets, Phys. Rev. B **85**, 094514 (2012); R. Monaco, arXiv:1203.6091.
[32] M. R. Samuelsen and S. A. Vasenko, J. Appl. Phys. **57**, 110 (1985).
[33] Y. M. Zhang and P. H. Wu, J. Appl. Phys. **68**, 4703 (1990).